

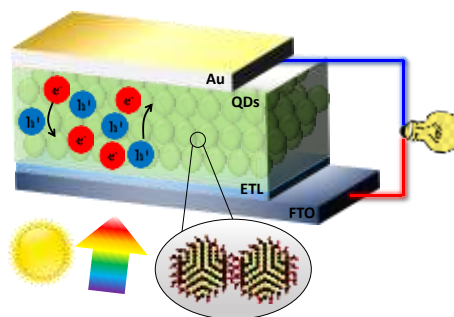
Accounts of Materials & Surface Research

Interface Engineering and Charge Carrier Management for Improving the Efficiency of Quantum Dot Solar Cells

Qing Shen*, Chao Ding, Dong Liu

Faculty of Informatics and Engineering, The University of Electro-Communications
1-5-1 Chofugaoka, Chofu-shi, Tokyo 182-8585, Japan
shen@pc.uec.ac.jp

Colloidal quantum dot (CQD) solar cell has attracted much interest as a next-generation solar cell because of its low cost and potential to surpass the Shockley–Queisser limit. However, the current power conversion efficiency (PCE) of CQD solar cells remains significantly below its theoretical limit, highlighting the need for fundamental research. The main challenges in improving the PCE include inefficient charge transport and extraction, as well as high non-radiative recombination at the device interfaces. This report reviews recent breakthroughs in enhancing CQD solar cell PCE through interface engineering and charge carrier management.



Keyword: PbS, quantum dot, solar cell, interface passivation, photoexcited carrier dynamics

Qing Shen graduated with a bachelor's degree from the School of Physics at Nanjing University in 1983 and earned a Ph.D. from the Graduate School of Engineering at the University of Tokyo in 1995. After graduation, he worked as an assistant at the Graduate School of Engineering at the University of Tokyo. From 1996, she became an assistant professor in the Department of Quantum and Matter Engineering at The University of Electro-Communications. Since 2016, she has been a professor at The University of Electro-Communications. Her research interest includes semiconductor nanomaterials and their application in optoelectronic devices, the study of photoexcited carrier dynamics using time-resolved laser spectroscopy, and fundamental research on new types of solar cells.



Chao Ding completed the doctoral program in The University of Electro-Communications in 2018. After graduation, he became a project researcher at the University of Electro-Communications since 2020. His research interest is the development of new materials for solar power generation and ultrafast spectroscopy studies on the photophysics of colloidal nanocrystals.



Dong Liu received a Ph.D. from The University of Electro-Communications in 2024. After graduation, he became a research fellow at The University of Electro-Communications. His research interest is the photoexcited carrier dynamics in nanomaterials and solar cells.



Interface Engineering and Charge Carrier Management for Improving the Efficiency of Quantum Dot Solar Cells

Qing Shen*, Chao Ding, Dong Liu

Faculty of Informatics and Engineering, The University of Electro-Communications
1-5-1 Chofugaoka, Chofu-shi, Tokyo 182-8585, Japan

1. Introduction

Quantum dots (QDs) are semiconductor nanocrystals with sizes ranging from a few nanometers up to tens of nanometers. Colloidal quantum dots (CQDs) solar cells, which can be easily synthesized through chemical methods, are anticipated as a promising candidate for the next generation of low-cost and high-efficiency solar cells. When applying CQDs to photoelectric conversion devices, several features can be highlighted: (1) low cost can be achieved through solution-based fabrication methods, (2) the absorption spectrum can be controlled by adjusting the size of the quantum dots, (3) the quantum confinement effect enhances the light absorption coefficient, and (4) the possibility of achieving a photocurrent quantum efficiency exceeding 100% due to multiple exciton generation (MEG). If the effect of MEG in point (4) can be fully utilized, the power conversion efficiency (PCE) of solar cells is predicted to surpass the Shockley-Queisser (S-Q) limit (~30%) and potentially reach a theoretical limit of 44%.¹ CQD solar cell device structures include wet-sensitized types and solid-state heterojunction/homojunction types.^{2,3,4} We have summarized the efficiencies and advantages of some mainstream QDs solar cells in Table 1. While their PCE has significantly improved over the past few years,

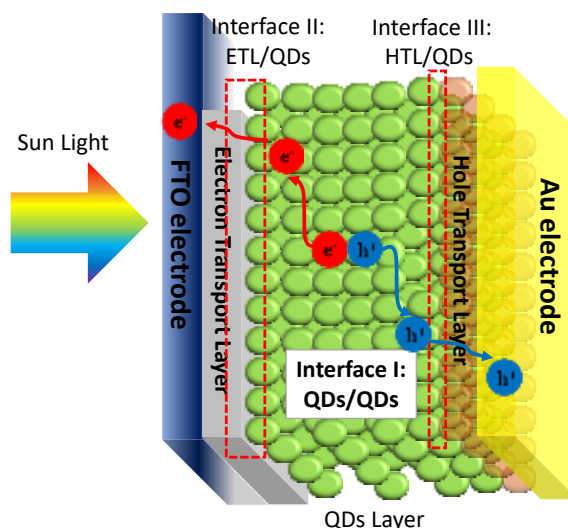


Figure 1. The device structure of heterojunction CQD solar cells and a schematic diagram of the three types of interfaces (QDs/QDs interface (Interface I), electron transport layer/quantum dot (ETL/QDs) interface (Interface II), and quantum dot/hole transport layer (QDs/HTL) interface (Interface III)).

it still remains below 20%, far from the theoretical conversion efficiency.^{2,3}

To further enhance the PCE of CQD solar cells, the following aspects are critical: (1) reduction of defects in CQDs, (2) adequate control of the various interface states of nanoparticles and construction of optimal charge separation interfaces, (3) suppression of charge recombination, (4) a thorough understanding of the MEG mechanism, and the establishment of methods to efficiently generate multiple excitons and extract them

Table 1. The PCE and advantages of mainstream QDs solar cells.

	QDs	PCE (%)	Advantages
<i>Ternary QDs</i>	AgBiS ₂	9.17 ⁵	High absorption coefficient Environmentally friendly
<i>Binary QDs</i>	PbS	15.45 ¹⁹	Tunable electronic properties Excellent environmental stability
	PbSe	11.60 ⁶	Large exciton Bohr radius Tunable bandgap (0.3~2 eV)
<i>Perovskite QDs</i>	FAPbI ₃	18.10 ^{7,8}	High ambient stability Long carrier lifetime Narrow band gap ($\approx 1.5\text{eV}$)
	Cs _x FA _{1-x} PbI ₃	17.29 ⁹	Preferable tolerance factors
	CsPbI ₃	16.64 ¹⁰	Tunable surface chemistry
<i>QD sensitized</i>	ZCISSe	16.10 ¹¹	Facile and low-cost fabrication Superior stability High defect tolerance

externally.¹² As shown in Table 1, as a traditional QDs material, lead sulfide (PbS) exhibits better environmental stability compared to other emerging QDs materials and is highly promising for next-generation photovoltaic applications. This paper focuses on recent research on PbS heterojunction CQD solar cells, discussing charge separation and carrier transport in CQD solar cells. The reduction of electron and hole defect densities through interface passivation, the extension of carrier diffusion length, improvement in charge extraction efficiency, and mechanisms for enhancing the photoelectric conversion properties of CQD solar cells have also been discussed.

2. The device structure and photoelectric conversion mechanism of CQD solar cells

Figure. 1 shows a schematic diagram of the structure of a heterojunction CQD solar cell device. Generally, it consists of an electron transport layer (ETL) (such as ZnO, SnO₂, or TiO₂), a light-absorbing layer of QDs several

hundred nanometers thick, and a hole transport layer (HTL) (such as a p-type QD layer or organic carrier transport materials). The electron-hole pairs generated by light absorption in the QD layer are separated into charges and collected by the electrodes at both ends through the ETL and HTL. In this process of charge separation, transport, and collection, the photogenerated carriers must pass through three types of interfaces: the quantum dot/quantum dot (QDs/QDs) interface (Interface I), the electron transport layer/quantum dot (ETL/QDs) interface (Interface II), and the quantum dot/hole transport layer (QDs/HTL) interface (Interface III). Therefore, interface engineering and the control of photogenerated carrier dynamics in heterojunction CQD solar cells are key to improving their photoelectric conversion properties. Recent advancements in improving the efficiency of CQD solar cell devices have been driven by innovations in CQD synthesis methods, exploration of

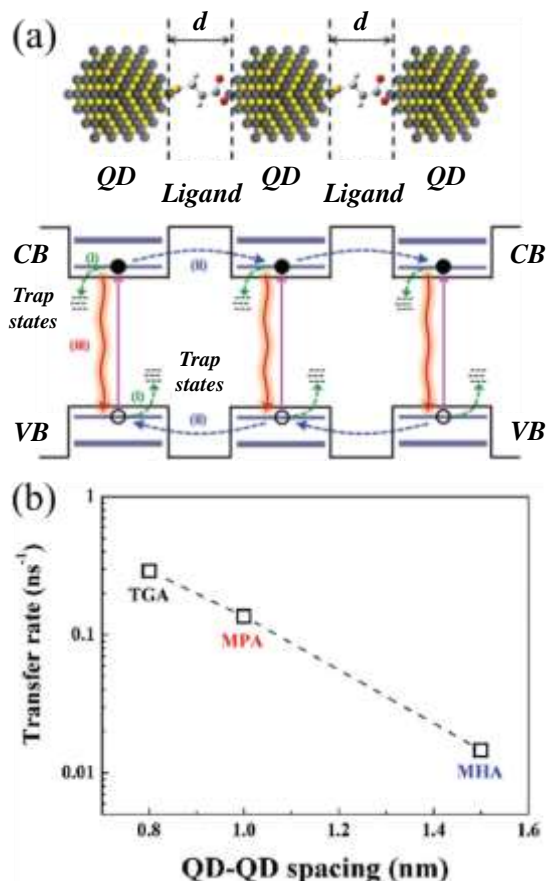


Figure 2. (a) A schematic diagram of the relaxation processes of photoexcited carriers in the CQD film. The main processes include (i) charge trapping, (ii) charge transfer between adjacent QDs, and (iii) radiative recombination. The solid and hollow dots in the figure represent photogenerated electrons and holes, respectively. (b) The dependence of the charge transfer rate constant between QDs on the QD-QD distance in the QD film. TGA (thioglycolic acid), MPA (3-mercaptopropionic acid), and MHA (6-mercaphohecanoic acid) are mercaptoalkanoic acid (MAA) ligands with different alkyl chain lengths. (Ref. 20) Reprinted with permission from Ref. 20. Copyright 2016, Royal Society of Chemistry.

different surface ligand exchanges, interface passivation techniques, and alignment of interface energy levels, all of which are rooted

in the precise control of these three interfaces.¹³⁻¹⁸

In our recent research, we found that controlling and passivating the three interfaces in PbS CQD solar cells led to a significant suppression of non-radiative recombination, along with the promotion of charge transport and a substantial improvement in the balance of electron and hole extraction. As a result, the PCE of PbS CQD solar cells reached 15.45%.¹⁹

3. QDs/QDs interface

The promotion of charge separation and charge transport of photoexcited carriers in the QD film, which serves as the light-absorbing layer in CQD solar cells, as well as the suppression of non-radiative charge recombination, is crucial for improving photoelectric conversion properties. To stabilize CQDs in a solvent, long alkyl chain organic ligands (such as oleic acid or oleylamine) are connected onto the surface of the CQDs. However, QD films formed by spin coating become electrically insulating due to these long-chain ligands. Therefore, when forming the QD light-absorbing layer, the long-chain ligands must be replaced with shorter organic ligands or inorganic ligands, such as halide ions. The ligand exchange on the QD surface is expected to achieve two main effects: (1) shortening the distance between QDs, which increases electronic coupling between adjacent QDs, and (2) reducing the interfacial defect density through passivation of the QDs/QDs interface. Through (1), charge transfer between QDs is enhanced, and through (2), non-radiative charge recombination at the QD interface is reduced. Using transient absorption (TA) spectroscopy, we evaluated the relaxation

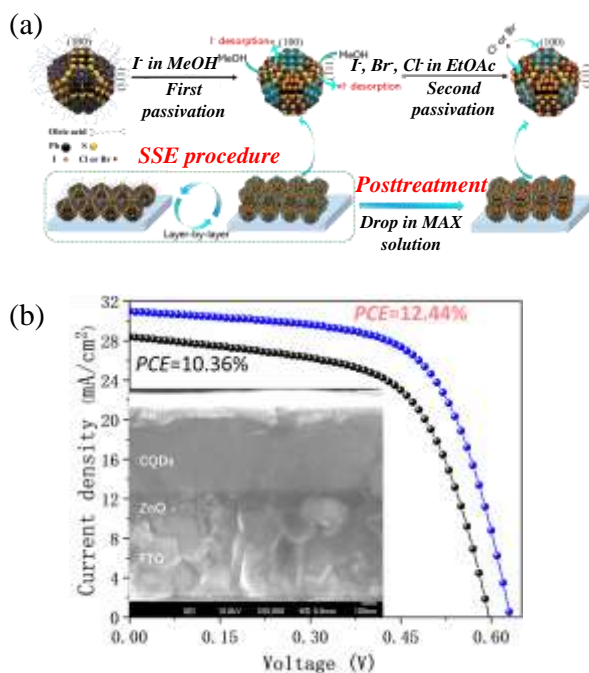


Figure 3. (a) The schematic diagram showing the film deposition process through solid-state ligand exchange and MAX post-treatment. (b) The improvement of PCE of PbS QD solar cells resulting from the MAX post-treatment. Inset: the SEM cross-sectional image of PbS QD solar cell. (Ref. 16) Reprinted with permission from Ref. 16. Copyright 2020, American Chemical Society.

dynamics of photogenerated carriers in QD films and found that they primarily involve charge trapping due to defects, charge transfer between adjacent QDs, and radiative recombination (Figure 2(a)).²⁰ By comparing the photogenerated carrier dynamics in QD films passivated with four different mercaptoalkanoic acid (MAA) ligands with varying alkyl chain lengths, we discovered that the charge transfer rate constant between QDs increases exponentially as the distance between QDs decreases (as the ligand chain length decreases) (Figure 2(b)). (Because the MHDA ligand is relatively long, the QD-QD spacing is comparatively large,

resulting in a TA signal that remains nearly constant within one nanosecond. As a result, carrier transfer does not occur between isolated QDs. Therefore, in Figure 2(b), only a comparison among the three shorter ligands is shown.) In charge transfer between QDs through tunneling or hopping, strong coupling between QDs is advantageous for the charge separation of photogenerated excitons (dissociation into electrons and holes) within QDs.²¹ Therefore, by minimizing the distance between QDs and enhancing QD coupling, the mobility of photogenerated carriers can be significantly improved. On the other hand, due to the high specific surface area, the coordination of atoms on the CQD surface is insufficient, leading to the formation of surface defect levels caused by many dangling bonds. While shallow defect levels can be used as dopants for QDs, deep defect levels act as centers for non-radiative recombination. Thus, surface defect levels affect the optical and electronic properties of QD films, but they can be reduced through proper passivation with suitable ligands.²² In recent years, the research and development of heterojunction CQD solar cells have made innovative progress, partly due to significant improvements in CQD surface ligand exchange technology.

In the heterojunction PbS CQD solar cells, ligand exchange is primarily performed using solid-state ligand exchange (SSLE) and liquid-state ligand exchange (LSLE) methods. In the SSLE method, after forming a QD film on a substrate through spin coating, the long ligands on the QD surface are replaced with shorter ligands. This process is repeated several times to form a QD light-absorbing layer with a thickness of several hundred

nanometers through a layer-by-layer method.

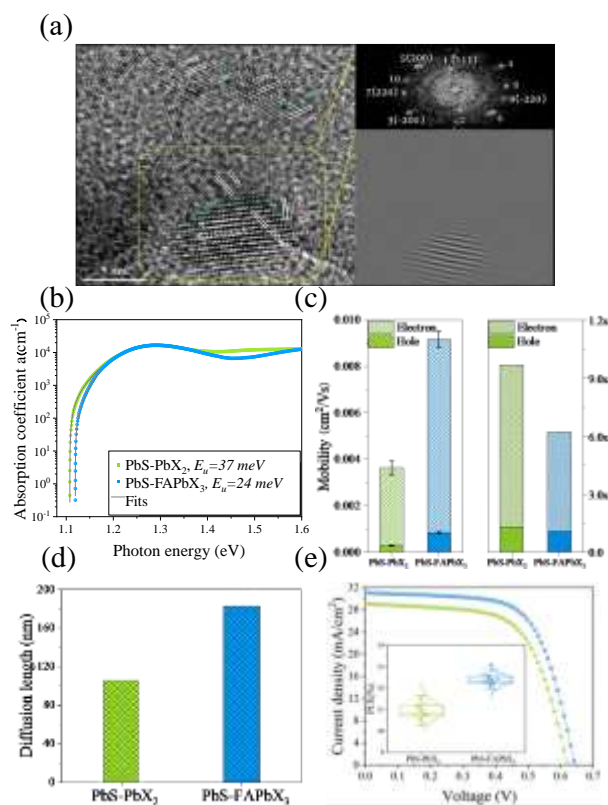


Figure 4. (a) TEM images of PbS-FAPbX₃ CQD films. The green dot lines represent the interface position roughly between the CQDs. Insets: The FFT phase diagram and the inverse FFT phase diagram of the corresponding HRTEM images are shown on the top right and bottom right, respectively. (b) Optical absorption spectra. (c) Comparison of carrier mobility and the trap density of electrons and holes in PbS-PbX₂ and PbS-FAPbX₃ CQD light-absorbing layers. (d) Comparison of carrier diffusion length. (e) Comparison of current density–voltage characteristics (under AM1.5G illumination) of PbS-FAPbX₃ and PbS-PbX₂ CQD solar cells (reference devices). (Inset: Comparison of energy conversion efficiency (PCE) of PbS-FAPbX₃ and PbS-PbX₂ CQD solar cells (reference devices)). (Ref. 12) Reprinted with permission from Ref. 12. Copyright 2022, Wiley.

Before 2017, SSLE was widely used. Initially, short-chain organic ligands were used to replace long-chain organic ligands in forming the QD film. In 2011, the Sargent et al. first used inorganic CdCl₂ and monovalent halide anions (Br) as ligands.²³ They not only replaced the long-chain organic ligands but also passivated the S²⁻ anions and Pb²⁺ cations exposed on the QD surface, leading to a reduction in the surface defect density of the PbS QD film. As a result, the QD films demonstrated improved stability in air and greater mobility of the photogenerated carriers. Since then, SSLE method based on replacing long-chain organic ligands with inorganic ligands and passivating the QD surface has become mainstream. For a long time, single halide ligands were used in SSLE, but it was difficult to completely passivate the entire PbS QD surface. To solve this problem, we proposed a simple two-step passivation approach (Figure 3(a)), where after replacing ligands with iodine (I) in SSLE, the formed PbS QD film was further treated with halide ligands (Cl, Br, or I). This post-treatment compensated for the deficiency of surface ligands, significantly reducing the defect density of the QD film and greatly improving charge transport. Compared with no post-treatment, the carrier diffusion length of the PbS QD film treated with Cl⁻ increased by 70%, and the PCE of the CQD solar cell improved from 10.36% to 12.44%. At that time, this PCE value was the highest achieved by PbS CQD solar cells fabricated using the SSLE method (Figure 3(b)). Furthermore, unencapsulated devices exhibited good stability in air.

On the other hand, in the LSLE method, the

ligand exchange process on the QD surface ink is then dispersed in solvents such as dimethylformamide (DMF), formamide (FA), or butylamine (BA). This allows for the one-step deposition of a QD film with a thickness of several hundred nanometers on a substrate via spin coating. Since the Sargent et al. proposed a ligand exchange method based on lead halide precursors and ammonium acetate stabilizers in 2017, the LSLE method has undergone groundbreaking changes, with the PCE of PbS CQD solar cells exceeding 11% for the first time.¹⁵ Compared to the SSLE method, LSLE allows for the deposition of QD films without exposing the CQD to air, thus preventing damage to the QD surface. Additionally, it effectively suppresses the introduction of hydroxyl groups (OH⁻) onto the CQD surface, leading to a reduction in surface defect density.²⁴

We have therefore developed a new method for fabricating PbS CQD ink using the LSLE method, which involves passivating the QD/QD interfaces with a perovskite monolayer. This approach aims to reduce the defect density in the PbS CQD light-absorbing layer and increase the lifetime and diffusion length of photogenerated carriers.¹¹ We prepared two types of inks for comparison: PbS-PbX₂ (X = I, Br) CQD ink and a new PbS-FAPbX₃ (FA = formamidinium, X = I, Br) CQD ink. For the former, PbS-PbX₂ CQD ink was formed by dispersing PbS CQD powder, obtained through ligand exchange in solution, directly into a mixture of amines (butylamine, pentylamine, and hexylamine) to obtain PbS CQD coated with two-dimensional lead halide monolayers (PbI₂ and PbBr₂). For the latter, PbS-FAPbX₃ CQD ink was prepared by

is carried out in solution. The exchanged QD dispersing PbS CQD powder into a mixture of formamidinium iodide (FAI) and amines to obtain PbS CQD coated with perovskite FAPbX₃ monolayers. After spin coating these PbS CQD inks to form films, we performed a heat treatment at 70°C for 5 minutes to remove the residual amines.

Transmission electron microscopy (TEM) observations of PbS-FAPbX₃ CQD films (Figure 4(a)) revealed the formation of a perovskite monolayer (FAPbX₃) on the surface of PbS CQDs, which facilitated the bridging of CQDs almost entirely along the (200) crystal plane. Analysis of the optical absorption spectra (Figure 4(b)) showed that the Urbach energy of the PbS-FAPbX₃ CQD film was 24 meV, which is 37% lower than that of the PbS-PbX₂ CQD film (37 meV). This indicates that the formation of the FAPbX₃ shell reduced the defect density in the PbS CQD film. Transient absorption (TA) measurements revealed that in the PbS-FAPbX₃ CQD films, the loss of charges due to charge trapping was reduced and an increase in the charge transfer rate constant between QDs was observed. Additionally, space-charge-limited current (SCLC) measurements showed a 40% reduction in defect density and a significant increase in carrier mobility in the PbS-FAPbX₃ CQD film compared to the PbS-PbX₂ CQD film (Figure 4(c)). The diffusion length of photogenerated carriers in the CQD film increased by 1.7 times (Figure 4(d)). As a result, the optimal thickness of the PbS-FAPbX₃ CQD light-absorbing layer increased by 11%, and the average PCE of the devices improved significantly from 10.95% to 12.39% compared to the PbS-PbX₂ CQD solar cells

(reference devices), with the highest PCE reaching over 13% (Figure 4(e)). The new method allowed for the simple formation of a monolayer perovskite $FAPbX_3$ shell on the PbS CQD surface, achieving increased carrier mobility and effective passivation of QDs/QDs interface defects. The subsequent sections will introduce further interface modifications at the ETL/QDs interface (Interface II) and QDs/HTL interface (Interface III), aiming to enhance PCE through the synergistic effects of modifying these two interfaces as well as all three interfaces.

4. ETL/QDs interface

In PbS CQD solar cells, the interface between the CQD light-absorbing layer and the n-type wide-bandgap metal oxides used as ETLs (e.g., ZnO, SnO_2 , TiO_2) is essential to suppress the backward movement of holes and ensure balanced transport of both electrons and holes. However, issues such as recombination of photogenerated carriers and photo-induced degradation at the ETL/QDs interface due to improper energy level alignment and interface defects have also been identified.²⁵ Therefore, the design and control of the ETL/QDs interface is a second key factor in improving the photovoltaic performance of CQD solar cells. The energy level alignment at this heterojunction interface directly influences carrier extraction, accumulation, and recombination at the interface. The energy levels of most ETLs, such as conduction band levels, can be controlled by doping. We systematically investigated the effect of adjusting the conduction band energy level of

the ZnO ETL by doping it with magnesium

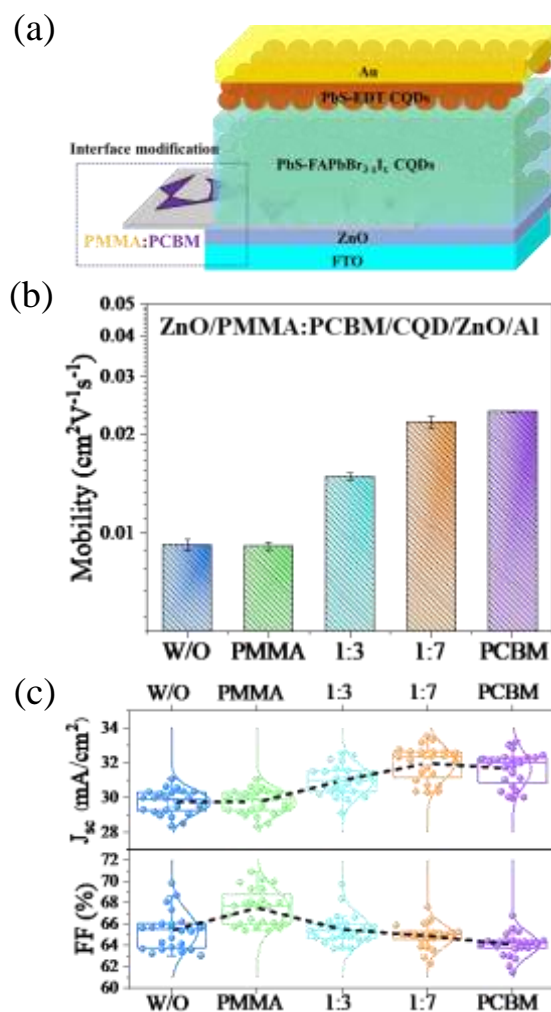


Figure 5. (a) A schematic diagram of a protective layer added at the ETL/QD interface. (b) Changes in electron mobility due to the passivation of the ZnO ETL/PbS QD interface (ETL/QDs, Interface II) and (c) variations in short-circuit current (J_{sc}) and fill factor (FF) of the CQD solar cell. (Ref. 12) Reprinted with permission from Ref. 12. Copyright 2022, Wiley.

($Zn_{1-x}Mg_xO$) and how these changes impact the photovoltaic performance of CQD solar cells.²⁶ It was found that shallow defect levels in $Zn_{1-x}Mg_xO$ ETLs can actually serve as injection pathways for photogenerated electrons from QDs to the ETL. Furthermore,

we discovered for the first time that the conduction band offset (CBO) between the ETL and QD film significantly influences interface recombination in CQD solar cells. When the CBO at the ETL/QDs interface forms a spike structure, charge recombination at the interface is significantly suppressed, leading to improved open-circuit voltage (V_{oc}) in CQD solar cells. Additionally, the energy levels at the ETL/QDs interface can be controlled using self-assembled monolayers (SAMs). Sargent et al. demonstrated that the introduction of negative dipole moment molecules between the ZnO ETL and the QD film effectively reduced the electron affinity of ZnO, achieving energy level alignment with the QD film and significantly improving both V_{oc} and fill factor (FF) of the CQD solar cells.²⁷

On the other hand, the defect density in the ETL also significantly affects charge recombination at the ETL/QDs interface. Currently, the metal oxide ETLs commonly used in CQD solar cells are all fabricated via low-temperature solution processes, which inevitably introduce many defects. To further improve the PCE of the aforementioned PbS-FAPbX₃ CQD solar cells, we chemically modified the ZnO ETL/QDs interface.¹⁹ One of the main issues at this interface is that the strong alkalinity of the solvent used in the PbS CQD ink for forming the QD film damages the ZnO nanoparticle film, which serves as the ETL layer, thereby increasing the interface defect density. As a protective layer for the ETL/QDs interface, we introduced a PMMA (polymethyl methacrylate) layer (about 10 nm) (Figure 5(a)). We found that PMMA not only prevented damage to the ETL film but also reduced interface defects. Furthermore, to

enhance the conductivity of the PMMA layer, we mixed PCBM into the PMMA film and

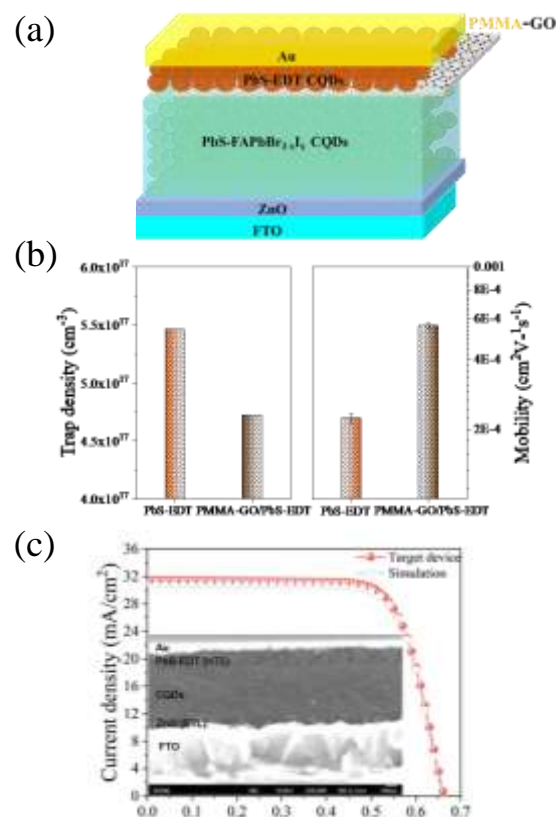


Figure 6. (a) A schematic diagram of introduction of PMMA-GO layer at the HTL/QD interface. (b) Reduction of trap state density and increase in hole mobility at the PbS-EDT HTL/PbS QD interface (Interface III) through PMMA-GO passivation. (c) J-V characteristics of PbS CQD solar cells with passivation at Interfaces I, II, and III (PCE: 15.45%, FF: 0.74, JSC: 31.5 mA/cm², V_{oc} : 0.66 V). (Ref. 12) Reprinted with permission from Ref. 12. Copyright 2022, Wiley.

introduced the mixed film (PMMA) at the interface. Increasing the PCBM content improved the electron extraction efficiency at the ETL/QDs interface and increased electron mobility within the device (Figure 5(b)). As a result, J_{sc} has been significantly improved, enhancing the photovoltaic performance of the device with the PMMA

(1:7) passivation layer. However, the maximum PCE only increased from 13.10% to 13.75% due to a decrease in FF. This result indicates that improving the FF is also crucial. (Figure 5(c)). Through the evaluation of photoexcited carrier dynamics and the simulation of the device's photovoltaic characteristics, we investigated the causes of the FF reduction. While the chemical modification of the ETL/QDs interface increased electron transport speed, it also exacerbated the difference between electron and hole transport speeds. As a result, the imbalance in electron and hole extraction within the device worsened, leading to hole accumulation at the QDs/HTL interface, which created a potential barrier unfavorable for hole transport. Consequently, the device's series resistance (R_s) increased, and shunt resistance (R_{sh}) decreased, both of which are critical factors contributing to the degradation of the device's FF. To address this issue, as discussed below, it is necessary to simultaneously control the QDs/HTL interface.

5. HTL/QDs interface

In heterojunction CQD solar cells (Figure 1), there are two heterojunction interfaces: ETL/QDs and QDs/HTL. Among these, the QDs/HTL interface is the most critical in PbS CQD solar cells. Introducing a hole transport layer (HTL) between the QD layer and the metal electrode not only promotes charge separation and hole extraction while suppressing the recombination of electrons in the reverse direction but also reduces the Schottky barrier between the QD layer and the metal electrode, benefiting the improvement of V_{OC} , J_{SC} , and FF. Therefore, the QDs/HTL interface is the third key factor

for enhancing the photovoltaic performance of CQD solar cells. Research on the QDs/HTL interface has primarily focused on the construction of HTLs.

Due to the tunable energy levels of CQDs, which can be adjusted based on their size and surface ligands, the most commonly used HTL in PbS CQD solar cells is a QD layer formed with CQDs of different sizes or ligands from those used in the light-absorbing layer. This type of HTL does not need to address the lattice matching issue at the QDs/HTL interface and can be fabricated using a layer-by-layer spin coating process.^{28,29} We investigated the impact of different HTL structures, formed by combining QD layers with four different sizes of QDs, on the photovoltaic performance of PbS CQD solar cells.²⁸ The results showed that this HTL structure exhibits a quantum funnel effect, meaning that photogenerated electrons near the HTL are efficiently transferred to the ETL side. This improved charge collection efficiency, leading to a significant increase in J_{SC} (over 20%).

In 2014, Bawendi et al. utilized the difference in energy levels between PbS CQDs passivated with iodine (I-PbS CQDs) and PbS CQDs passivated with ethanedithiol (EDT-PbS CQDs). They used an EDT-PbS QD layer as the HTL, significantly improving V_{OC} , J_{SC} , and FF through increased charge collection efficiency.³⁰ Currently, p-type QD layers passivated with small molecule ligands containing thiol functional groups are the most commonly used HTLs in PbS CQD solar cells.²⁹

Therefore, to further enhance the PCE of the PbS-FAPbX₃ CQD solar cells mentioned in Sections 3 and 4, we conducted chemical

modifications on the interface between the QD light-absorbing layer and the HTL (EDT-

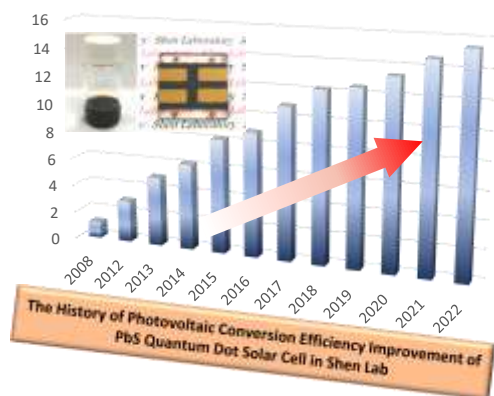


Figure 7. The history of PCE progress of PbS CQDs solar cells in Shen Lab of UEC.

PbS QDs) (interface III). To improve the balance between electron extraction and hole extraction and reduce QDs/HTL interface defects, we introduced a PMMA-GO layer (a mixed layer of PMMA and graphene oxide (GO) with hole transport properties) between the n-type PbS QD layer (light-absorbing layer) and the p-type PbS QD layer (HTL) (Figure 6(a)). When depositing the p-type QD layer as the HTL on top of the QD absorbing layer, the strong polar acetonitrile solvent used caused some ligands on the surface of the QD absorbing layer to detach, introducing interface defects. In our study, forming a PMMA-GO layer on the surface of the QD absorbing layer before depositing the HTL not only effectively protected the QD absorbing layer but also reduced the interface defect density due to the passivation effect of PMMA (Figure 6(b)). More importantly, the introduction of the PMMA-GO layer significantly improved hole mobility (Figure 6(b)). As a result, the hole extraction efficiency at the QDs/HTL interface increased, and the balance between the transport and collection of electrons and holes was

improved. Consequently, the FF was increased to over 70%, while maintaining a high J_{SC} (>30 mA/cm²) and a high V_{OC} (0.66 V). By engineering all three interfaces (I, II, and III) simultaneously, we achieved a PCE of 15.45% (FF: 0.74; J_{SC} : 31.5 mA/cm²; V_{OC} : 0.66 V) (Figure 6(c)). This PCE is the highest reported for single-junction PbS CQD solar cells. The synergistic effect of modifying all three interfaces is evident compared to modifying a single interface or two interfaces (Figure 6(c)). Additionally, these devices retained more than 90% of their initial PCE after being stored in dry air for over 160 days, demonstrating good air storage stability. The synergistic passivation approach for the three interfaces in CQD solar cells not only provides new ideas for improving the photovoltaic performance of CQD solar cells but can also be applied to other heterojunction solar cells and LEDs, paving the way for high-performance optoelectronic devices in future.

6. Summary and outlook

Based on the systematic fundamental research in the interface engineering and photogenerated carrier dynamics, the PCE of CQD solar cells in our laboratory has made significant progress, reaching a world-class level (Figure 7). It is believed that to further enhance the PCE of CQD solar cells and surpass the Shockley-Queisser limit, research in the following three areas is necessary and crucial:

(1) The research and development of QD light-absorbing layers with excellent optical and electronic properties are extremely important for further improving the photovoltaic performance of CQD solar cells.

The formation and utilization of QD bulk heterojunctions (BHJs) based on a blend of n-type and p-type QDs appear to be a promising approach.

(2) To improve the photoelectric characteristics and stability of traditional p-type QDs passivated with thiol ligands, new ligands and passivation methods need to be proposed.

(3) Adequately controlling the three aforementioned interfaces and achieving a balanced charge transfer throughout the entire CQD solar cell device are key to further improving the PCE. Therefore, it is necessary to carefully consider the appropriate electron and hole transport layers, as well as the mobility of electrons and holes in the QD light-absorbing layer.

In the near future, research and development based on these important points are expected to lead to significant breakthroughs in the PCE of CQD solar cells.

5. Acknowledgement

This research was partially supported by JSPS KAKENHI (Grant Numbers 20H02565, 26286013).

Reference

- Hanna, M.C., et al., *J. Appl. Phys.* **2006**, *100* (7) 074510.
- Song, H., et al., *J. Am. Chem. Soc.* **2021**, *143* (12) 4790-4800.
- NREL (2021). Best Research-Cell Efficiency Chart. <https://www.nrel.gov/pv/cell-efficiency.html>.
- Ma, W., et al., *Adv. Mater.* **2022**, *34*, 2105977.
- Wang, Y, et al., *Nat. Photon.* **2022**, *16*, 235–241.
- Yuan, M., et al., *Small.* **2022**, *18*, 2205356
- Aqoma, H., et al., *Nat. Energy.* **2024**, *9*, 324–332.
- Zhang, X., et al., *Angew. Chem. Int. Ed.* **2023**, *62*, e202214241
- Jia, D., et al., *Adv. Mater.* **2023**, *35*, 2212160.
- Jia, D., et al., *Energy Environ. Sci.*, **2022**, *15*, 4201-4212.
- Zhang, Z., et al., *ACS Energy Lett.* **2023**, *8*, 1, 647–656.
- Sogabe, T., et al., *J. Photonics Energy.* **2016**, *6* (4) 040901.
- Wang, Y., et al., *Nat. Commun.* **2019**, *10* (1) 5136.
- Wang, Y., et al. *Adv. Mater.* **2018**, *30* (16) e1704871.
- Liu, M., et al., *Nat. Mater.* **2017**, *16* (2) 258.
- Ding, C., et al., *ACS Energy Lett.* **2020**, *5* (10) 3224.
- Choi, M.-J., et al., *Nat. Commun.* **2020**, *11* (1) 103.
- Xu, J., et al., *Nat Nanotechnol.* **2018**, *13* (6) 456.
- Ding, C., et al., *Adv. Energy Mater.* **2022**, *12* (35) 2201676.
- Chang, J., et al., *Phys. Chem. Chem. Phys.* **2017**, *19* (9) 6358.
- Hu, L.L., et al., *J. Appl. Phys.* **2021**, *129* (9) 091101.
- Kagan, C.R., et al., *Science.* **2016**, *353* (6302) aac5523.
- Tang, J., et al., *Nat. Mater.* **2011**, *10* (10) 765.
- Aqoma, H., et al., *Adv. Mater.* **2017**, *29* (19) 1605756.
- Liu, J., et al., *Adv. Mater.* **2021**, *33* (29) e2008115.
- Ding, C., et al., *Nanoscale Horizon.* **2018**, *3* (4) 417.
- Kim, G.-H., et al., *Nano Letter.* **2015**, *15* (11) 7691.
- Ding, C., et al., *ACS Appl. Mater. Interfaces.* **2018**, *10* (31) 26142.
- Yuan, M., et al., *Nat. Energy.* **2016**, *1* (3) 16016.
- Chuang, et al., *Nat. Mater.* **2014**, *13* (8) 796.